Title	Flow-induced Alignment of Amyloid Protofilaments Revealed by Linear Dichroism
Author(s)	Adachi, Rumi; Yamaguchi, Kei-ichi; Yagi, Hisashi et al.
Citation	Journal of Biological Chemistry. 2007, 282(12), p. 8978-8983
Version Type	VoR
URL	https://hdl.handle.net/11094/71289
rights	
Note	

Osaka University Knowledge Archive : OUKA

https://ir.library.osaka-u.ac.jp/

Osaka University

Flow-induced Alignment of Amyloid Protofilaments Revealed by Linear Dichroism*⑤

Rumi Adachi[‡1], Kei-ichi Yamaguchi[‡1,2], Hisashi Yagi[‡], Kazumasa Sakurai[‡], Hironobu Naiki[§], and Yuji Goto[‡3]

From the [‡]Institute for Protein Research, Osaka University and CREST, Japan Science and Technology Agency, Yamadaoka 3-2, Suita, Osaka 565-0871, Japan and [§]Department of Pathological Sciences, Faculty of Medical Sciences, University of Fukui and CREST, Japan Science and Technology Agency, Matsuoka, Fukui 910-1193, Japan

Amyloid fibrils underlying various serious amyloidoses including Alzheimer and prion diseases form characteristic deposits in which linear fibrils with an unbranched and rigid morphology associate laterally or radially, *e.g.* radial senile amyloid plaques of amyloid β. To clarify the formation of these high order amyloid deposits, studying the rheology is important. A 22-residue K3 peptide fragment of β₂-microglobulin, a protein responsible for dialysis-related amyloidosis, forms long and homogeneous protofilament-like fibrils in 20% (v/v) 2,2,2-trifluoroethanol and 10 mM HCl (pH ~2). Here, using circular dichroism and linear dichroism, we observed the flow-induced alignment of fibrils. Analysis of far- and near-UV linear dichroism spectra suggested that both the net π-π^* transition moment of the backbone carbonyl group and L_b transition moment of the Tyr[26] side chain are oriented in parallel to the fibril axis, revealing the structural details of amyloid protofilaments. Moreover, the intensities of flow-induced circular dichroism or linear dichroism signals depended critically on the length and type of fibrils, suggesting that they are useful for detecting and characterizing amyloid fibrils.

Although the structural features of amyloid fibrils are of urgent importance (1–3), the high molecular weight and noncrystalline assembly preclude the use of conventional methods, such as x-ray crystallography or multidimensional NMR, to acquire high resolution structural images. Recently, it has been found that amyloid fibrils are, in general, amenable to the magic angle-spinning solid-state nuclear magnetic resonance methods, providing a general view of the atomic level structure in which β-strands are stacked in a parallel and registered manner (4–6). A structure revealed by x-ray diffraction of a crystalline short amyloidogenic peptide was consistent with this view (7).

More recently, the mechanical characterization of individual fibrils by atomic force microscopy revealed that the insulin fibrils have a strength and stiffness comparable with that of steel and silk, respectively (8). Among various structural features, although the long and rigid morphology of amyloid fibrils might be responsible for their biological consequences, rheological details remain unknown.

β₂-Microglobulin (β2-m),[4] a typical immunoglobulin domain made of 99 residues, is a target of extensive study because of its clinical importance and suitable size for examining the relationship between protein folding and amyloid formation (9–14). Dialysis-related amyloidosis is a common and serious complication among patients on long term hemodialysis, in which amyloid fibrils of β2-m deposit in the synovia of the carpal tunnel (9, 15). A 22-residue K3 peptide, corresponding to Ser[20]–Lys[41] of β2-m forms protofilament-like fibrils in various solvents including a low concentration of 2,2,2-trifluoroethanol (16–19). Although the efficient fibrillation of intact β2-m requires seeding, K3 forms fibrils spontaneously. Furthermore, K3 formed two types of fibrils (known as f218 and f210) differing in the amounts of β-sheet and morphology (18, 19). The f210 fibrils are remarkably long with a thin and homogeneous morphology, whereas the f218 fibrils are short and thick and apparently heterogeneous. f210 fibrils may provide an excellent model with which to study the rheology of amyloid fibrils. In this paper, we have shown that circular dichroism (CD) and linear dichroism (LD) are useful for detecting the flow-induced alignment fibrils. By analyzing the flow-induced LD, we address the structure and viscoelastic properties of amyloid fibrils.

EXPERIMENTAL PROCEDURES

Proteins and Amyloid Fibrils—Recombinant human β2-m was expressed and purified using the *Escherichia coli* expression system as described previously (20). K3 was obtained by digestion of β2-m with lysyl endopeptidase (*Achromobacter* protease I) as reported previously (16).

β2-m amyloid fibrils were formed by the fibril extension method as reported previously (20), in which the fragmented fibrils were extended by the monomeric proteins. First, a solution of monomeric β2-m at 25 μM (0.3 mg ml⁻¹) in 50 mM

---

glycine buffer (pH 2.5) and 100 mM NaCl was prepared, and then β2-m seeds (sonicated amyloid fibrils) were added to the monomeric solution to a final concentration of 0.42 μM (5 μg ml^{-1}). Hereafter, the concentration of seeds or fibrils is expressed in terms of molar concentration of monomers, because the size of seeds or fibrils was difficult to define. This solution was incubated overnight at 37 °C.

f210 and f218 fibrils were formed by the fibril extension method established by Yamaguchi *et al.* (18). To make f210 fibrils, K3 peptide was first dissolved in 10 mM NaOH at 1 mM and then diluted 10-fold in 20% (v/v) 2,2,2-trifluoroethanol and 11 mM HCl to a concentration of 100 μM. The final concentration of HCl was adjusted to 10 mM, 1 mM NaCl was produced by neutralization, and f210 seeds were added to the monomeric solution to a final concentration of 3 μM (7.5 μg ml^{-1}). To make f218 fibrils, K3 peptide was dissolved directly in 20% (v/v) 2,2,2-trifluoroethanol and 10 mM HCl at a final concentration of K3 of 100 μM without seeds. The peptide solutions were incubated overnight at 25 °C. Amyloid fibrils were extended without agitation, and the conformational change was monitored by far-UV CD spectroscopy.

CD and LD Measurements—Standard CD measurements without flow were performed with a Jasco J-600 spectropolarimeter at 25 °C. Far-UV CD spectra were measured using a cell with a light path of 1 mm, and the concentration of amyloid fibrils was 25 μM. The results were expressed as the mean residue ellipticity (θ) (deg cm^2 dmol^{-1}).

To perform the CD measurements under flow, we installed a quartz flow cell with a light path of 2 mm (Fig. 1*A*). Temperature was not controlled, and the measurements were at room temperature. The concentrations of amyloid fibrils were 5.1 and 103 μM for the far- and near-UV CD measurements, respectively. Using a tubing pump, the fibril solution was circulated at a flow rate of 1.16 ml min^{-1} during the measurements. In the vertical cell setting, the solution was flowed from bottom to top. We confirmed that the flow-induced signals of K3 fibrils are not caused by the high photomultiplier voltage under flow (data not shown). We also confirmed that globular monomer proteins do not exhibit the flow-induced signal change (see supplemental Fig. S1). Furthermore, flow-induced signals were observed with other CD spectropolarimeters (data not shown), confirming that the observation was not caused by an artifact of the machine's calibration.

LD measurements were performed with a Jasco J-720 spectropolarimeter equipped with an LD mode, using a quartz flow cell with a light path of 2 mm at room temperature (Fig. 1*A*). In the far-UV LD measurements, the concentrations of f210, f218, and β2-m fibrils were 5.1, 5.0, and 2.5 μM, respectively. In the near-UV LD measurements, the concentrations of f210, f218, and β2-m fibrils were 103, 100, and 25 μM, respectively. The results were expressed as the molar absorption coefficient ϵ (cm^{-1} M^{-1}).

Electron and Atomic Force Microscopy Measurements—The sample solutions were diluted 20-fold with distilled water. These diluted samples were spread on copper grids (400 mesh) covered by carbon-coated collodion film and allowed to stand for 1 min. After the removal of excess solution with filter paper, the grids were negatively stained with a 2% (w/v) uranyl acetate solution. After staining for 1 min, the solution on the grids was removed with filter paper and dried. These samples were examined with a JEOL-100CX transmission electron microscope operated at 80 kV. Atomic force microscopy images were obtained using a NanoScope IIIa (Digital Instruments/Veeco) as described previously (18).

Ultrasonication Analysis—Fragmentation of amyloid fibrils was carried out by ultrasonicating 1-ml aliquots of a 103 μM f210 fibril stock solution using a Microson sonicator (Misonix, Farmingdale, NY) at an intensity level of 2 and with repeated 20-s pulses on ice. The number of pulses was 0, 1, 10, 20, and 30. Sedimentation velocity measurements of fragmented fibrils were performed with a Beckman-Coulter Optima XL-1 analytical ultracentrifuge as described previously (21).

RESULTS AND DISCUSSION

CD Measurement of f210 Fibrils under Flow—When we measured the far- and near-UV CD spectra of f210 fibrils, we noticed that the signal intensities fluctuated under certain conditions, suggesting that the flow critically affects the spectra. To characterize the effects of the flow, we measured the CD spectra under flow by installing a flow cell into the spectropolarimeter (Fig. 1*A*). Without a flow, f210 fibrils exhibited a CD spectrum with a minimum of ~210 nm and strong negative ellipticity, as was reported previously (18), probably reflecting the highly ordered cross-β structure (Fig. 1*B*). When the solution was flowed vertically (β = 90°), the spectrum changed to that with a maximum of ~196 nm and an immense positive ellipticity. In contrast, when f210 fibrils were flowed horizontally (β = 0°), the spectrum shifted to the opposite direction (Fig. 1*B*). The difference spectrum obtained by subtracting the spectrum without flow indicated that the induced CDs have the same intensity but with the opposite sign (Fig. 1*D*). A flow-induced CD signal was also observed in the near-UV region (Fig. 1*C*). Without flow, the f210 fibrils, containing Tyr[26], Phe[22], and Phe[30] as aromatic groups, exhibited a unique near-UV spectrum (18). When the solution was flowed vertically, the CD spectrum exhibited two positive peaks at 279 and 285.5 nm with strong ellipticities (Fig. 1*C*). When the solution was flowed horizontally, two negative peaks were observed, exactly the mirror image of the spectrum under vertical flow (Fig. 1*E*). We confirmed that these flow-induced signals were not caused by an artifact of the machine's calibration (see "Experimental Procedures" and supplemental Fig. S1). It is likely that the flow-induced LD contributed to the apparent CD signals (22).

LD Measurements of f210 Fibrils under Flow—LD had been used to investigate the orientation of absorbing chromophores within elongated molecules (23–28). Although chiral compounds generate CD signals, oriented compounds either intrinsically or during the measurements often exhibit LD signals. LD is defined by the difference in absorption of linearly polarized lights in parallel ($A_\parallel$) and perpendicular ($A_\perp$) to an orientation axis, given by the following.

$$LD = A_\parallel - A_\perp \qquad \text{(Eq. 1)}$$

With the machine we used, the plane of parallel polarized light was set to be horizontal, and that of perpendicularly polarized light was vertical (Fig. 1*A*). Thus, when the flow induced the
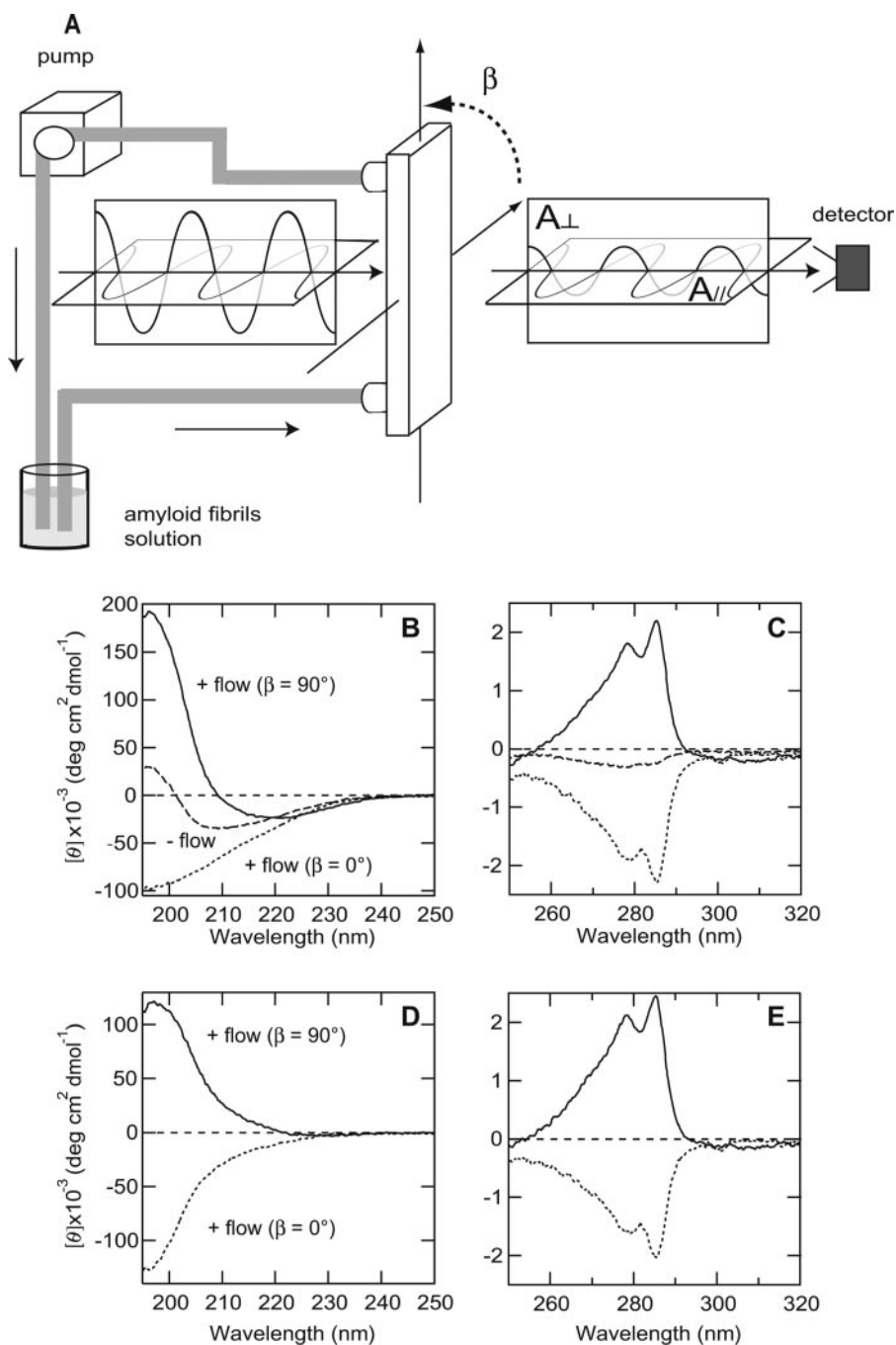
FIGURE 1. **Schematic diagram of the flow cell and flow-induced CD spectra.** *A*, schematic diagram of the flow cell system for CD and LD measurements. The diagram shows a case under vertical flow. Using a tubing pump, the solution of amyloid fibrils was circulated at a flow rate of 1.2 ml min^{-1} during the measurements. β is the angle of the cell from the front, relative to the horizon. With the spectropolarimeter used, the plane of linearly polarized light in parallel ($A_{\parallel}$) is horizontal and that of perpendicularly polarized light ($A_{\perp}$) is vertical. The flow-induced CD spectra of f210 fibrils. Far (*B*) and near (*C*) UV CD spectra were measured under vertical (*solid lines*) or horizontal (*dotted lines*) flows or without flow (*dashed lines*). Difference spectra in the far-UV (*D*) and near-UV (*E*) regions under vertical (*solid lines*) or horizontal (*dotted lines*) flows were obtained by subtracting the spectrum without flow.

flowed vertically ($\beta = 90°$), a spectrum with a minimum at 198.5 nm was observed. When the solution was flowed in oblique directions ($\beta = 45$ or $135°$), no significant spectrum was obtained; the absorption of polarized light parallel to an orientation axis was the same as that of perpendicularly polarized light, leading to the compensated LD spectrum. As for near-UV LD spectra, the sign of the LD signal was converted from positive to negative when the direction of flow was rotated by 90° (Fig. 2*B*), the same as the far-UV LD. These results are consistent with Equation 1, indicating that the flow-induced CD signals were indeed caused by the aligned f210 fibrils. In the subsequent LD experiments, we used the flow in the vertical direction ($\beta = 90°$), because it was easier to make a stable flow.

We then examined the dependence of LD signals on the flow rate (Fig. 2*F*). With an increase of the flow rate, the LD signal at 198.5 nm increased up to 1 ml min^{-1} and then gradually decreased. Considering this flow rate dependence, we performed the CD and LD measurements at a flow rate of 1.2 ml min^{-1}, where the LD signal was maximal. The largest molar absorption coefficient was $\sim 50 - 60 \times 10^3$ cm^{-1} M^{-1} on average. However, we observed significant variation ($\sim 30 - 80 \times 10^3$ cm^{-1} M^{-1}) depending on fibril preparations, suggesting that the length of fibrils, which was difficult to control precisely, critically affects the LD amplitude (see below). The results indicated that, although the flow induces the alignment of f210 fibrils and consequently LD, it saturates at a certain flow rate, and moreover, a flow rate that is too high decreases LD. Probably, at high flow rates, the breaking of fibrils by shearing forces or induction of tur-

alignment of fibrils in line with the direction of the flow, the sign of the LD signal was expected to be converted when the direction of flow was rotated by 90°.

We performed the far-UV LD measurements with the rotation of the flow cell every 45° (Fig. 2, *A* and *C*). When the solution was flowed horizontally ($\beta = 0°$), an LD spectrum with a maximum at 198.5 nm was observed. When the solution was

bulence decreased the degree of alignment. f210 fibrils often exhibited a relatively small LD ($\sim 10 \times 10^3$ cm^{-1} M^{-1}) even without flow, suggesting that f210 fibrils tended to align when the solution was introduced into the flow cell with a 2-mm light path (Fig. 2*F*).

Orientation of Functional Groups in Fibrils—The far-UV absorption spectrum of f210 fibrils is composed of two amide
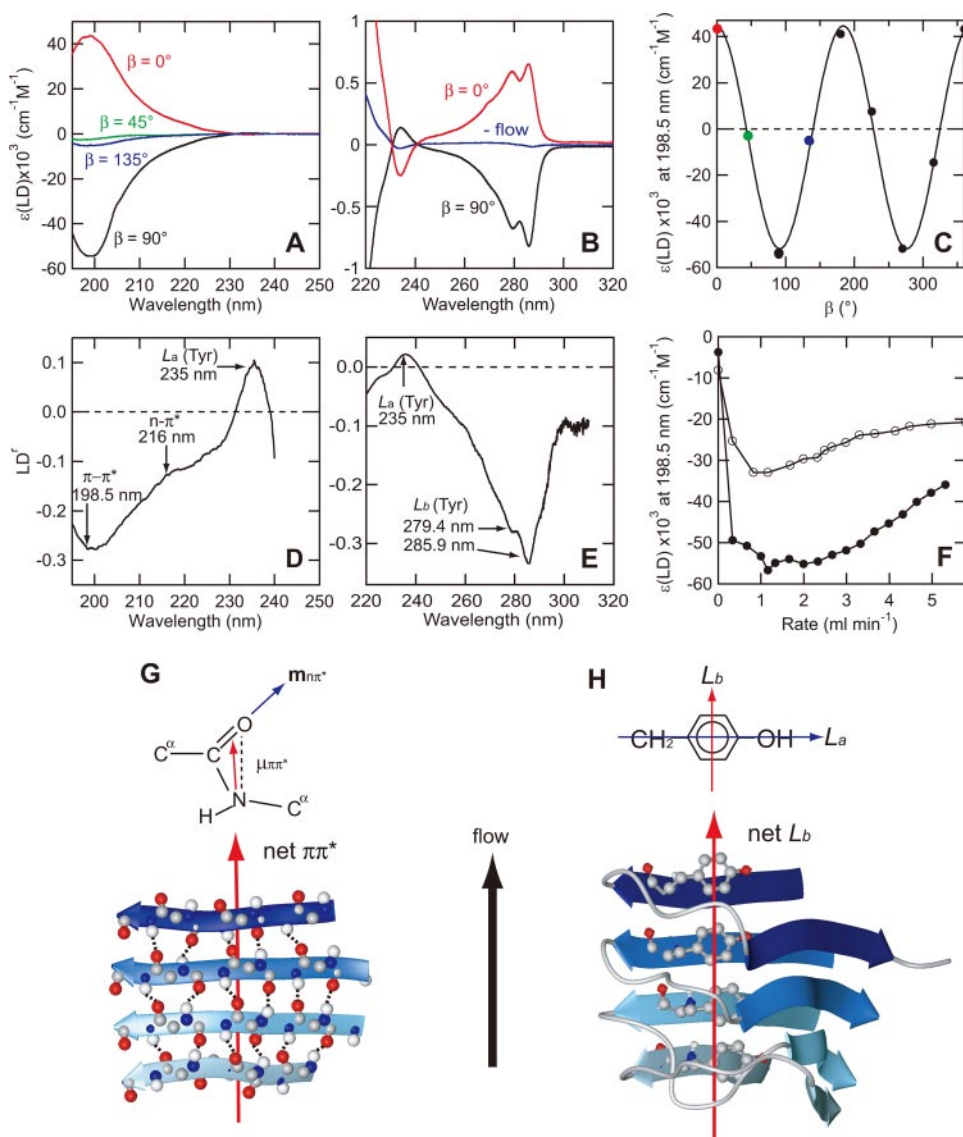
FIGURE 2. **The flow-induced LD spectra of f210 fibrils.** *A* and *B*, dependence of flow-induced LD on the direction of flow. *A*, far-UV LD spectra at various angles of the flow cell ($\beta = 0°$ (horizontal), 45°, 90° (vertical), and 135°). *B*, near-UV LD spectra at $\beta = 0°$, $\beta = 90°$, and without flow. *C*, dependence of $\epsilon(LD)$ at 198.5 nm on β. *Solid circles* are observed values, of which four points between 0 and 135° correspond to the spectra with the same color in *A*. LD^r spectra in the far-UV (*D*) and near-UV (*E*) regions, which were obtained by $\epsilon(LD)/\epsilon(UV)$. *F*, dependence of $\epsilon(LD)$ at 198.5 nm on the flow rate at $\beta = 90°$. The results for the two fibril preparations are shown. *G*, electric dipole transition moment of the amide $\pi\pi^*$ transition ($\mu_{\pi\pi^*}$), the magnetic dipole transition moment of the amide nπ^* transition (m$_{n\pi^*}$), and three-dimensional structural model of f210 fibrils representing an ordered backbone with net $\pi\pi^*$ transition moments parallel to the fibril axis. *H*, the transition moments of tyrosine chromophores and three-dimensional structural model representing ordered Tyr[26] side chains. The Tyr side chain has two transition moments; one is L_a with $\epsilon_{max} = \sim 10^4$ M^{-1} cm^{-1} near 230 nm, and the other is L_b with $\epsilon_{max} = \sim 1,400$ M^{-1} cm^{-1} at ~ 280 nm. The LD^r spectrum suggests that the L_b transition moment of Tyr[26] contributes most to the observed LD^r.

π-π^* transition moments of carbonyl groups at 198 nm are known to be parallel to the C=O bond axis or perpendicular to β-strands in the plane of the β-sheet (24, 25, 27–29) (Fig. 2*G*). In other words, net π-π^* transition moments are expected to be parallel to the fibril axis ($\alpha \approx 0°$; see below). In contrast, net n-π^* transition moments are not fixed and of low intensity (24, 25, 29). The negative sign of the LD band at 198.5 nm for the vertical flow (Fig. 2*A*, $\beta = 90°$) means that perpendicularly polarized light is absorbed more than parallel polarized light ($A_{\parallel} < A_{\perp}$). Thus, the observed negative LD at 198 nm indicates that net π-π^* transition moments are aligned in line with the direction of flow, in agreement with the expectation that the elongated fibrils are oriented to the direction of flow. A similar suggestion was also reported based on the flow-induced far-UV LD spectrum of amyloid β-(1–42) (24, 25).

A quantitative estimate of the orientation of the fibrils can be made by reduced LD (LD^r),

$$LD^r = \frac{LD}{A} = \frac{3}{2}S(3\cos^2\alpha - 1)$$

(Eq. 2)

where A is the absorption of the fibrils, S is the orientation factor that defines the efficiency of the fibril orientation ($S = 1$ and 0 for perfect and random orientations, respectively), and α is the angle that the transition moment makes with the orientation axis (23–28). The reduced LD spectrum indicated a dominant peak at 198.5 nm with LD$^r = -0.28$ (Fig. 2*D*). Although α should be near to 0°, the exact value is unknown. Thus, we plotted the correlation between S and α (supplemental Fig. S3), suggesting that the orientation factor of f210 fibrils is $\sim 0.09 - 0.1$.

A similar discussion can be applied to the near-UV LD. Although the Phe side chain also has two transition moments at 210 and 260 nm, the LD^r spectrum with two minima at 279 and 285 nm suggests that the L_b transition moment of Tyr[26] contributes most to the observed LD^r (Fig. 2*E*). The observed negative LD^r means that perpendicularly polarized light is absorbed by the L_b transition moment more than parallel polarized light ($A_{\parallel} < A_{\perp}$). Because the direction of flow is vertical,

chromophores at 198 and 216 nm, which were fitted by Gaussian functions (supplemental Fig. S2). The chromophores at 198 and 216 nm were assigned to a net amide π-π^* transition moment and net n-π^* transition moment of carbonyl groups of the backbone, respectively (24, 25, 27–29). For each peptide bond, the electric dipole transition moment of the amide π-π^* transition (μ_{π-π^*}) is directed approximately along the NO direction, whereas the magnetic dipole transition moment of the amide n-π^* transition ($m_{n-\pi^*}$) is directed along the carbonyl bond (Fig. 2*G*) (29). On the other hand, in the β-sheet, net
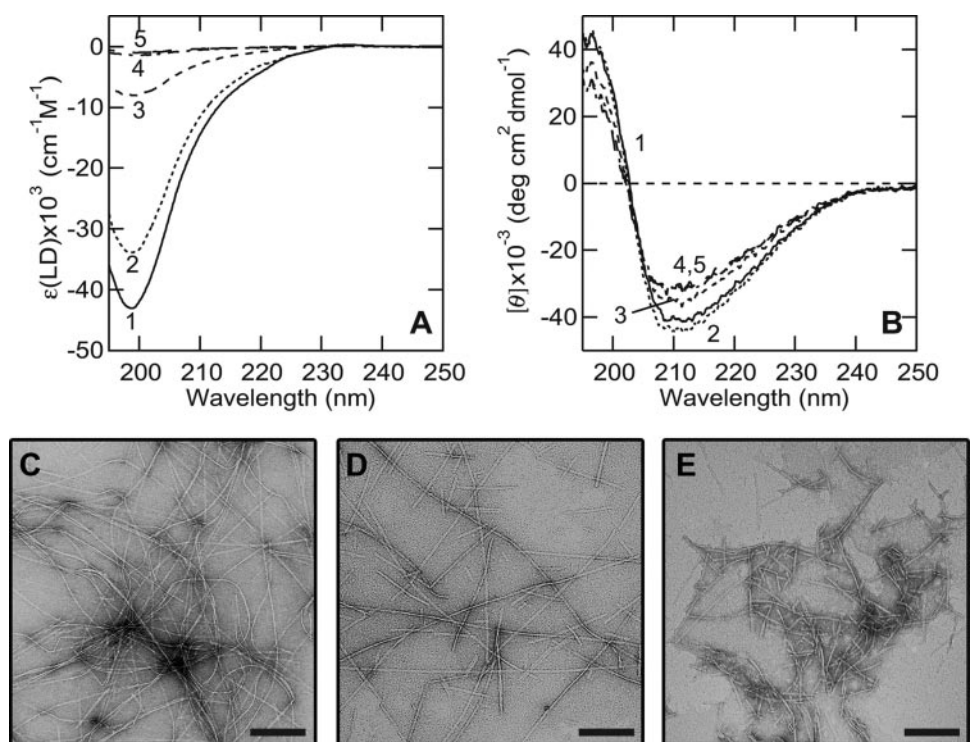
FIGURE 3. **Dependence of LD on the length of f210 fibrils.** The number of ultrasonication pulses applied was 0 (*trace 1*), 1 (*trace 2*), 10 (*trace 3*), 20 (*trace 4*), and 30 (*trace 5*). *A*, far-UV LD spectra under vertical flow. *B*, far-UV CD spectra without flow. Shown also are electron microscopy images of f210 fibrils without ultrasonication (*C*), after 10 pulses (*D*), and after 30 pulses (*E*) of ultrasonication. The *scale bars* in *C*–*E* represent 200 nm.
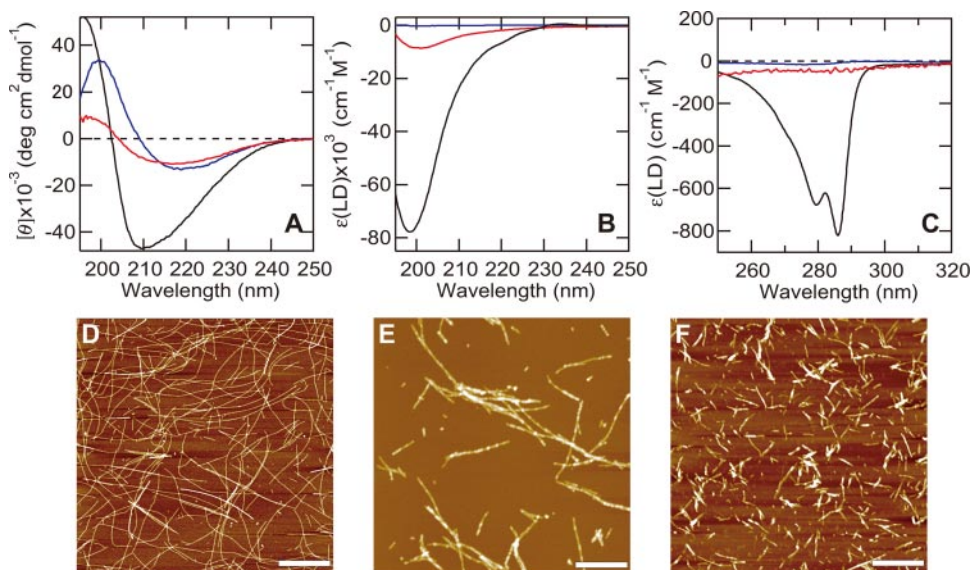

FIGURE 4. **Comparison of the flow-induced LD spectra of different fibrils.** Shown are far-UV CD (*A*), far-UV LD (*B*), and near-UV LD (*C*). Fibrils studied are mature β2-m fibrils (*red*), f218 fibrils (*blue*), and f210 fibrils (*black*). Shown also are atomic force microscopy images of f210 (*D*), β2-m (*E*), and f218 (*F*) fibrils. The *scale bars* in *D*–*F* represent 1 μm.

the overall L_b transition moment is polarized parallel to the direction of the fibril axis as illustrated in Fig. 2*H*. To address the side chain conformation, the relation between S and α at LD^r = -0.3 was plotted, as was the case of the main chain net π-π^* transition moment (supplemental Fig. S3). Although we can define neither S nor α values, it is reasonable to expect that the orientation factor S of the side chain is smaller than those of the π-π^* transition moment of car-

bonyl groups ($S = 0.09{\sim}0.1$), suggesting that α of the L_b transition moment is in the region of $\alpha < 20°$ (supplemental Fig. S3).

Correlation between the Flow-induced Alignment and Length of Fibrils—We found that ultrasonication treatment decreases the LD signal (Fig. 3*A*). For the samples with 20 and 30 pulses of ultrasonication (20 s for each pulse), no LD signal was detected. Sedimentation velocity measurements showed that, although the original f210 fibrils have a broad distribution of the sedimentation coefficient ($s_{20,w}$) above 35, ultrasonication pulses break the fibrils, producing fragmented short fibrils without producing monomers (data not shown). Electron microscopy images confirmed the ultrasonication-dependent fragmentation, leading to fibrils of ~500 nm (Fig. 3, *C*–*E*). On the other hand, the CD spectrum was independent of ultrasonication pulses showing that the total amount of β-sheet did not depend on the treatment (Fig. 3*B*). In Equation 2, because α is invariable, the orientation factor S decreases as fragmentation proceeds. Thus, as with other rod-like polymers, flow-induced orientation critically depends on fibril length. From electron microscopy images, it is assumed that a length of >500 nm is required to exhibit the flow-induced alignment and, consequently, the LD signal. Intriguingly, in a study with DNA, it was reported that the order of 1000 base pairs (~340 nm in length, the same as the length of K3 fibrils) is required to exhibit significant flow LD (27).

To examine the generality of the flow-induced alignment, we measured the LD in flow of β2-m mature fibrils at pH 2.5 and f218 fibrils in 20% (v/v) 2,2,2-trifluoroethanol at pH ~2.0. These fibrils showed far-UV CD spectra typical of a β structure (Fig. 4*A*). Although the LD signal of β2-m fibrils was stronger than that of f218 fibrils, it was much weaker than that of f210 fibrils in both far- and near-UV regions (Fig. 4, *B* and *C*). We observed no flow-induced CD signal for these samples. In apparent length, the order of fibrils is f210 fibrils > β2-m fibrils > f218 fibrils (Fig. 4, *D*–*F*), confirming that the length is a dominant factor determining the flow-induced LD.

CONCLUSIONS

Although the conditions are non-physiological, the results presented here indicate that LD will become a unique approach to addressing the rheological and structural features of amyloid fibrils. The responses of fibrils to the flow should depend on morphology, including length, width, viscoelastic properties, and interfibrillar interactions. Clarifying these features will be important for understanding how *in vivo* the intrinsically linear amyloid fibrils interact with each other to eventually form characteristic and organized lateral or radial clusters such as senile amyloid plaques (1–3, 30). The sensitivity of flow-induced LD or CD was not high for relatively short and thick fibrils such as β2-m mature fibrils and K3 f218 fibrils. However, it will be possible to increase the sensitivity by tuning the flow cell (24) or manipulating the solvent conditions, and then, either with CD or LD, the flow-induced alignment might become an important method for sensitively detecting and characterizing amyloid fibrils.

Finally, CD spectra generally represent the secondary or tertiary structures of proteins in the far- and near-UV regions, respectively (29). However, considering the highly ordered morphology and resultant unique CD spectrum as seen for f210 fibrils even in the absence of flow, a conventional analysis of secondary structure on the basis of CD data for globular proteins cannot be used. Such an approach will lead to an overestimation of α-helical content. On the other hand, several previous studies have suggested that the LD signals are included in the observed CD signals, when CD measurements of oriented substances are performed (22). Here, starting with the effects of flow on the CD spectra, we have established the flow-induced LD of K3 fibrils. We do not understand the mechanism by which unique CD signals are produced by the flow-induced alignment of fibrils. A hint to resolving this issue comes from the observations that spectral shapes were similar between LD and CD in both far- and near-UV regions, but the signs were opposite. Clarifying this issue and CD and LD spectroscopies of amyloid fibrils will further our understanding of the structural and spectroscopic features of amyloid fibrils.

REFERENCES

1. Dobson, C. M. (2003) *Nature* **426,** 884–890
2. Lansbury, P. T., Jr. (2004) *Nat. Med.* **10,** 13709–13715
3. Hardy, J., and Selkoe, D. (2002) *Science* **297,** 353–356
4. Ritter, C., Maddelein, M., Siemer, A. B., Luhrs, T., Ernst, M., Meier, B. H., Saupe, S. J., and Riek, R. (2005) *Nature* **435,** 844–848
5. Petkova, A. T., Yau, W., and Tycko, R. (2006) *Biochemistry* **45,** 498–512
6. Iwata, K., Fujiwara, T., Matsuki, Y., Akutsu, H., Takahashi, S., Naiki, H., and Goto, Y. (2006) *Proc. Natl. Acad. Sci. U. S. A.* **103,** 18119–18124
7. Nelson, R., Sawaya, M. R., Balbirnie, M., Madsen, A., Riekel, C., Grothe, R., and Eisenberg, D. (2005) *Nature* **435,** 773–778
8. Smith, J. F., Knowles, T. P., Dobson, C. M., MacPhee, C. E., and Welland, M. E. (2006) *Proc. Natl. Acad. Sci. U. S. A.* **103,** 15806–15811
9. Jahn, T. R., and Radford, S. E. (2005) in *Amyloid Proteins, The Beta Sheet Conformation and Disease* (Sipe, J. D., ed) pp. 667–695, Wiley-VCH Verlag, Weinheim, Germany
10. Jahn, T. R., Parker, M. J., Homans, S. W., and Radford, S. E. (2006) *Nat. Struct. Mol. Biol.* **13,** 195–201
11. Eakin, C. M., Berman, A. J., and Miranker, A. D. (2006) *Nat. Struct. Mol. Biol.* **13,** 202–208
12. Relini, A., Canale, C., De Stefano, S., Rolandi, R., Giorgetti, S., Stoppini, M., Rossi, A., Fogolari, F., Corazza, A., Esposito, G., Gliozzi, A., and Bellotti, V. (2006) *J. Biol. Chem.* **281,** 16521–16529
13. Ivanova, M. I., Sawaya, M. R., Gingery, M., Attinger, A., and Eisenberg, D. (2004) *Proc. Natl. Acad. Sci. U. S. A.* **101,** 10584–10589
14. Hoshino, M., Katou, H., Hagihara, Y., Hasegawa, K., Naiki, H., and Goto, Y. (2002) *Nat. Struct. Biol.* **9,** 332–336
15. Gejyo, F., Yamada, T., Odani, S., Nakagawa, Y., Arakawa, M., Kunitomo, T., Kataoka, H., Suzuki, M., Hirasawa, Y., Shirahama, T., Cohen, A. S., and Schmid, K. (1985) *Biochem. Biophys. Res. Commun.* **129,** 701–706
16. Kozhukh, G. V., Hagihara, Y., Kawakami, T., Hasegawa, K., Naiki, H., and Goto, Y. (2001) *J. Biol. Chem.* **277,** 1310–1315
17. Ohhashi, Y., Hasegawa, K., Naiki, H., and Goto, Y. (2004) *J. Biol. Chem.* **279,** 10814–10821
18. Yamaguchi, K., Takahashi, S., Kawai, T., Naiki, H., and Goto, Y. (2005) *J. Mol. Biol.* **352,** 952–960
19. Yamaguchi, K., Naiki, H., and Goto, Y. (2006) *J. Mol. Biol.* **363,** 279–288
20. Chiba, T., Hagihara, Y., Higurashi, T., Hasegawa, K., Naiki, H., and Goto, Y. (2003) *J. Biol. Chem.* **278,** 47016–47024
21. Kihara, M., Chatani, E., Sakai, M., Hasegawa, K., Naiki, H., and Goto, Y. (2005) *J. Biol. Chem.* **280,** 12012–12018
22. Davidsson, Å., Nordén, B., and Seth, S. (1980) *Chemical Physics Letters* **70,** 313–315
23. Marrington, R., Seymour, M., and Rodger, A. (2006) *Chirality* **18,** 680–690
24. Dafforn, T. R., Rajendra, J., Halsall, D. J., Serpell, L. C., and Rodger, A. (2004) *Biophys. J.* **86,** 404–410
25. Dafforn, T. R., and Rodger, A. (2004) *Curr. Opin. Struct. Biol.* **14,** 541–546
26. Marrington, R., Dafforn, T. R., Halsall, D. J., and Rodger, A. (2004) *Biophys. J.* **87,** 2002–2012
27. Rodger, A., and Nordén, B. (1997) *Circular Dichroism and Linear Dichroism*, Oxford University Press, Oxford
28. Rodger, A., Rajendra, J., Marrington, R., Ardhammer, M., Norden, B., Hirst, J. D., Gilbert, A. T. B., Dafforn, T. R., Halsall, D. J., Woolhead, C. A., Robinson, C., Pinheiro, T. J. T., Kazlauskaite, J., Seymour, M., Perez, N., and Hannon, M. J. (2002) *Phys. Chem. Chem. Phys.* **4,** 4051–4057
29. Woody, R. W. (1996) in *Circular Dichroism and the Conformational Analysis of Biomolecules* (Fasman, G. D., ed) pp. 25–67, Plenum Press, New York
30. Jin, L., Claborn, K., Kurimoto, M., Geday, M., Maezawa, I., Sohraby, F., Estrada, M., Kaminsky, W., and Kahr, B. (2003) *Proc. Natl. Acad. Sci. U. S. A.* **100,** 15294–15298

Flow-induced Alignment of Amyloid Protofilaments Revealed by Linear Dichroism

Rumi Adachi, Kei-ichi Yamaguchi, Hisashi Yagi, Kazumasa Sakurai, Hironobu Naiki
and Yuji Goto

Access the most updated version of this article at doi: 10.1074/jbc.M611738200

Alerts:
- When this article is cited
- When a correction for this article is posted

Click here to choose from all of JBC's e-mail alerts

Supplemental material:
http://www.jbc.org/content/suppl/2007/01/30/M611738200.DC1

This article cites 21 references, 9 of which can be accessed free at
http://www.jbc.org/content/282/12/8978.full.html#ref-list-1

FLOW-INDUCED ALIGNMENT OF AMYLOID PROTOFILAMENTS REVEALED BY LINEAR DICHROISM*

Rumi Adachi, Kei-ichi Yamaguchi, Hisashi Yagi, Kazumasa Sakurai, Hironobu Naiki, and Yuji Goto
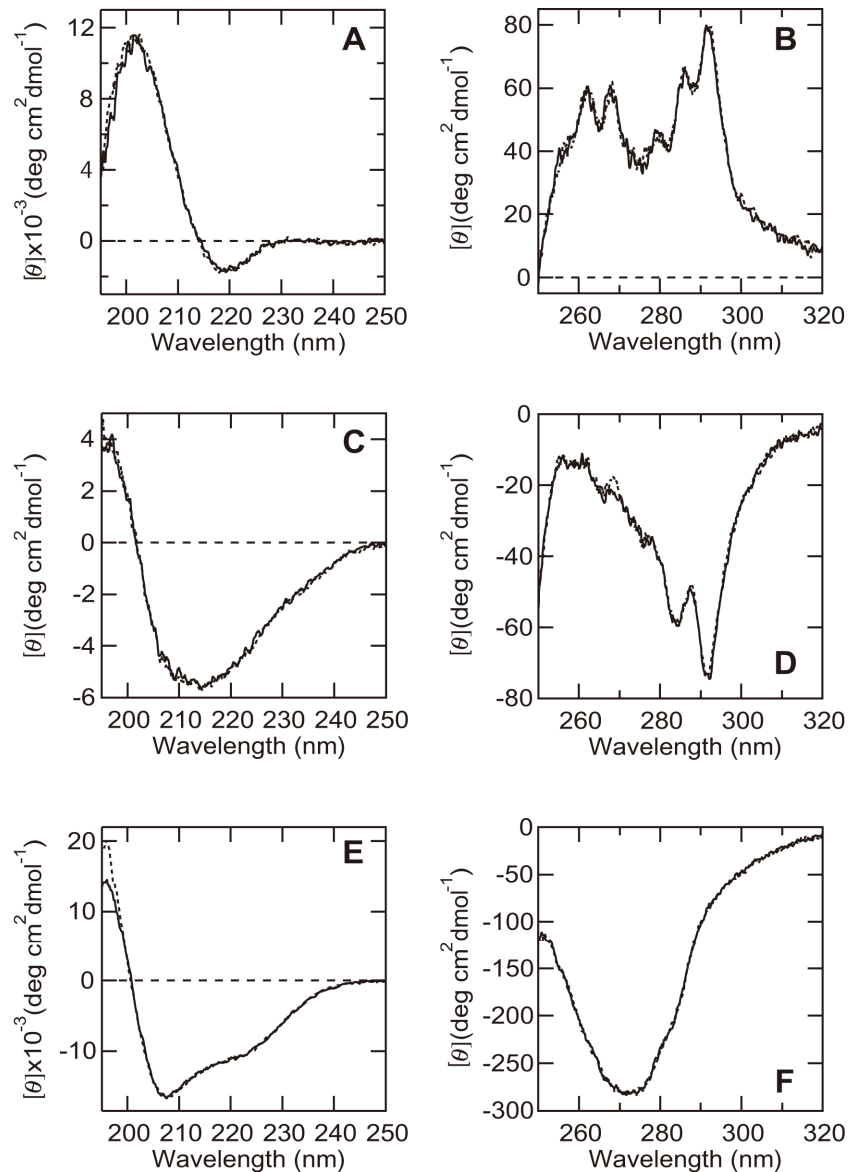

SUPPLEMENTAL FIGURE 1. **The flow-induced CD spectra of the native monomeric proteins.** β2-m (A, B) at pH 7.0, bovine β-lactoglobulin (C, D) at pH 7.0, and bovine insulin (E, F) at pH 2.0. Far-UV (A, C, E) and near-UV (B, D, F) CD spectra were measured under vertical flow (solid line) or without flow (dotted line), revealing no flow-induced CD for the native states.
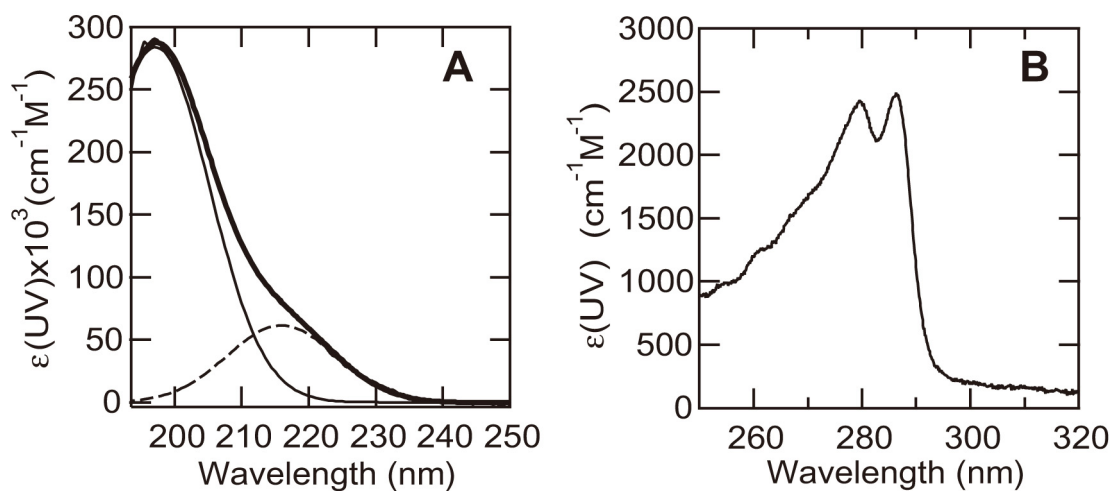
SUPPLEMENTAL FIGURE 2. **The far-UV (A) and near-UV (B) absorption spectra of f210 fibrils.**
The far-UV spectrum was separated into two components: π-π^* transition moments with a maximum at
198 nm (solid line) and n-π^* transition moments with a maximum at 216 nm (dash line). Far-UV
absorption spectra were measured at room temperature with a Hitachi U-3000 spectrophotometer, using a
cell with a light-path of 2 mm. The concentration of f210 fibrils was 5.1 μM. Near-UV absorption
spectra were measured using a cell with a light-path of 1 cm. The concentration of f210 fibrils was 100
μM.
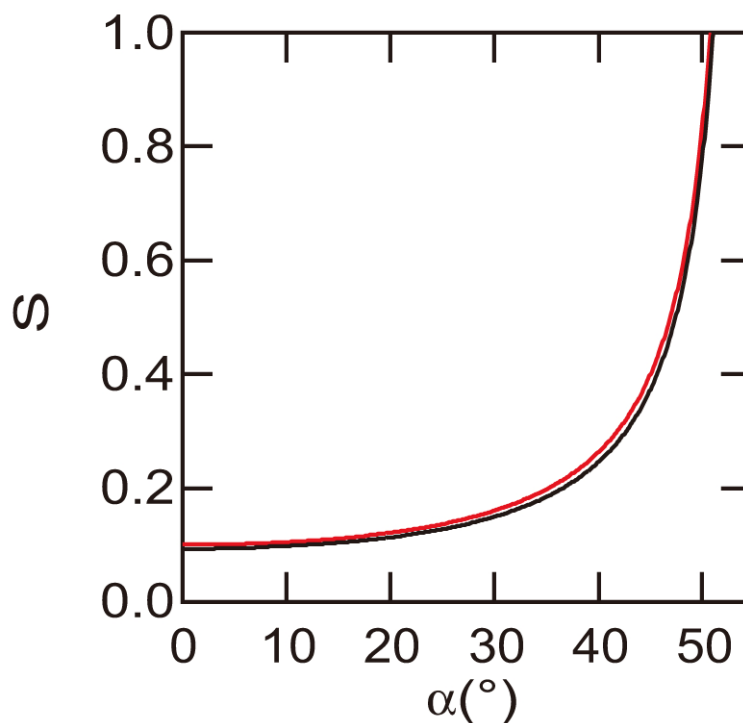
SUPPLEMENTAL FIGRURE 3. **The correlations between S and α of the π-π* transition moment of carbonyl groups (black lines) and L_b transition moment of Tyr26 (red lines) assuming the LD^r to be 0.28 and 0.30, respectively.** It is noted that the observed negative LD^r signals mean that perpendicularly polarized light was absorbed by both the π-π* and L_b transition moments more than the horizontally polarized light. Because the direction of flow is vertical, these transition moments are polarized parallel to the direction of the fibril axis. Here, following a conventional definition that LD is the difference in absorption of light linearly polarized parallel and perpendicular to an orientation axis, we assumed the positive values for the LD^r. If we assume that the net π-π* transition moments of carbonyl groups are polarized in parallel to the fibril axis (i.e., $\alpha = 0°$), S is 0.093. If we assume $\alpha = 20°$, S is ~0.1. These considerations suggest that the orientation factor of f210 fibrils is 0.09 ~ 0.1. As for the L_b transition moment of Tyr26, the correlation suggests that S and α are in the regions of $\alpha < 20°$ and $S < 0.1$, respectively.